

Valid Two-Sample Graph Testing via Optimal Transport Procrustes and Multiscale Graph Correlation: Applications in Connectomics

Jaewon Chung^{a,†}, Bijan Varjavand^{a,†}, Jesús Arroyo^{a,b}, Anton Alyakin^a, Joshua Agterberg^a, Minh Tang^c, Carey E. Priebe^a, Joshua T. Vogelstein^{a,*}

Abstract. Testing whether two graphs come from the same distribution is of interest in many real world scenarios, including brain network analysis. Under the random dot product graph model, the nonparametric hypothesis testing framework consists of embedding the graphs using the adjacency spectral embedding (ASE), followed by aligning the embeddings using the median flip heuristic, and finally applying the nonparametric maximum mean discrepancy (MMD) test to obtain a p-value. Using synthetic data generated from *Drosophila* brain networks, we show that the median flip heuristic results in an invalid test, and demonstrate that optimal transport Procrustes (OTP) for alignment resolves the invalidity. We further demonstrate that substituting the MMD test with multiscale graph correlation (MGC) test leads to a more powerful test both in synthetic and in simulated data. Lastly, we apply this valid and more powerful test to the right and left hemispheres of the larval *Drosophila* mushroom body brain networks, and conclude that there is not enough evidence to reject the null hypothesis that the two hemispheres are equally distributed.

Keywords: Random dot product graph, distance correlation, brain networks, *Drosophila* mushroom body.

1 Introduction A network, or graph, is a data type which naturally encodes information about relationships between variables. Statistical network analysis is becoming an increasingly important area [1], as it has applications in fields such as brain [2] and social sciences [3]. Often, we encounter more than one graph observation, and it is scientifically interesting to determine whether the two graphs come from the same distribution: the *two-sample graph hypothesis testing* problem. When the two samples are real-valued scalars, procedures such as the *t*-test and Wilcoxon rank-sum test are available, but these methods do not generalize to more complex data types such as graphs.

Recently, methods have been proposed for determining whether two graphs are statistically equivalent under different settings [4–14]. Most of these methodologies are aimed for pairs of graphs with a known correspondence between their vertices, and thus the problem consist in finding significant differences on the corresponding edges or vertices. Here, we focus on the more general setting where this vertex correspondence is unknown or might not exist, for example when the graphs do not have the same number of vertices. In this setting, we are interested in identifying significant differences on some underlying structure on the vertices. In particular, Tang et al. [6] proposed a nonparametric approach able to operate on pairs of graphs in which there is no known correspondence between their corresponding vertex sets using on the concept of distance between probability distributions on a vertex latent space. This method uses the maximum mean discrepancy (MMD) test to detect differences between distributions of the estimated latent positions of the vertices. In Agterberg et al. [15], the authors extend this procedure to resolve the inherent non-identifiabilities in the vertex latent space via an optimal transport solution that yields consistent nonparametric hypothesis testing.

MMD has been shown to be equivalent to the Energy distance two-sample test, the Hilbert-Schmidt independence criterion (HSic), and the distance correlation test for independence (DCorr) [16, 17]. HSic and DCorr, which are independence tests, are used as two-sample tests via first performing a

*Corresponding author: jovo@jhu.edu; †These authors contributed equally

^aJohns Hopkins University, Baltimore, MD 21218, United States

^bUniversity of Maryland, College Park, MD 20742, United States

^cNorth Carolina State University, Raleigh, NC 27695, United States

k-sample transform, which consists of concatenating the two samples, defining an auxiliary label vector, and subsequently testing for independence of those [17]. Multiscale graph correlation (MGC) is a recently proposed measure of dependence that has shown an improved empirical power in many settings by intelligently selecting the appropriate scale of the data [18–20]. In this paper, we propose a new methodology for equivalence of distribution between graphs that incorporates MGC as the test statistic. We demonstrate empirically in multiple simulation and synthetic data settings that MGC outperforms other methods, and demonstrate its use on the problem of comparing the connectivity of the brain hemispheres of the *Drosophila melanogaster*.

2 Background

2.1 Graphs and Embeddings A graph $G = (\mathbb{V}, \mathbb{E})$ with n vertices is composed of a vertex set $\mathbb{V} = \{v_1, \dots, v_n\}$ and an edge set $\mathbb{E} \subseteq \mathbb{V} \times \mathbb{V}$, where the edge $(v_i, v_j) \in \mathbb{E}$ connects vertices i and j . Graphs can be represented by an adjacency matrix $A \in \{0, 1\}^{n \times n}$, with rows and columns corresponding to vertices and matrix entries corresponding to edge values, so $A_{ij} = 1$ whenever $(v_i, v_j) \in \mathbb{E}$.

The *random dot product graph* (RDPG) model [21] treats the entries of an adjacency matrix A as independent Bernoulli random variables, where the probability of an edge is given by the dot product of pairs of latent positions $x_1, \dots, x_n \in \mathbb{R}^d$ for each vertex, so $\mathbb{P}(A_{ij} = 1) = x_i^\top x_j$. These latent positions are independent random variables sampled according to some distribution F . Writing $X = [x_1 \cdots x_n]^\top$ as the matrix of latent positions, we denote by $(X, A) \sim \text{RDPG}_n(F)$ a RDPG with adjacency matrix A and (usually unobserved) latent positions X sampled from F . With this notation, we have that $\mathbb{E}(A|X) = XX^\top$.

The RDPG model provides a flexible framework for studying the statistical equivalence of a pair of graphs. Suppose that $(X, A) \sim \text{RDPG}_n(F_X)$ and $(Y, B) \sim \text{RDPG}_m(F_Y)$. Then, the two graphs A and B are said to have the same distribution if there exists an orthogonal matrix $W \in \mathbb{R}^{d \times d}$, $W^\top W = I$ that makes X and $W^\top Y$ to have the same distribution. The matrix W accounts for the nonidentifiability inherent with inner products [6]. Formally, this hypotheses test can be stated as

$$\begin{aligned} H_0 : F_X &= F_Y \circ W && \text{for some orthogonal operator } W, \\ H_A : F_X &\neq F_Y \circ W && \text{for all orthogonal operators } W. \end{aligned}$$

Here, $F_Y \circ W$ denotes the distribution of the random variable $W^\top Y$. The graphs A and B do not need to have a correspondence between their vertices, or even the same number of vertices, because we are comparing distributions of latent positions instead of the latent positions themselves. This work focuses on cases where the number of vertices are equal, that is $n = m$.

Latent positions are typically unobserved in practice and can be estimated via the *adjacency spectral embedding* (ASE) [22]. Suppose that $A = USV^\top + U_\perp S_\perp V_\perp^\top$ is the singular value decomposition of A , where $U, V \in \mathbb{R}^{n \times d}$, $U_\perp, V_\perp \in \mathbb{R}^{n \times (n-d)}$ are jointly orthogonal matrices corresponding to the singular vectors of A , and $S \in \mathbb{R}^{d \times d}$, $S_\perp \in \mathbb{R}^{(n-d) \times (n-d)}$ are diagonal matrices such that S contains the d largest singular values of A . Then, the ASE of A is defined as $\hat{X} = US^{1/2}$. This simple and computationally efficient approach results in consistent estimates \hat{X} and \hat{Y} of the true latent positions X and Y [22–24]. If the two networks have different number of vertices, the difference in variance of the two estimates must be corrected since the subsequent testing procedure might be invalid [25].

The ASE depends on a parameter d that corresponds to the rank of the expected adjacency matrix conditionally on the latent positions; in practice, we estimate this dimension via the scree plot of the eigenvalues of the adjacency matrix which can be done automatically via a likelihood profile approach

[26].

2.2 Orthogonal Nonidentifiabilities There are two sources of an orthogonal nonidentifiability associated with using the ASE in RDPG [27]. The first is associated with the RDPG model itself, and can take a form of any orthogonal transformation, since for any orthogonal matrix W , it holds that $(XW)(XW)^\top = XWW^\top X^\top = XX^\top$. When using ASE, this orthogonal matrix converges to a population value at the rate $O_p(n^{-1/2})$, and, thus, rarely has any inferential consequences [6, 27].

The second source, called subspace nonidentifiability, is associated with taking a singular value decomposition as a part of the ASE. For the moment, consider the singular value decomposition of the matrix XX^\top . Since it is positive semidefinite, its eigendecomposition and singular value decomposition coincide. If XX^\top has no repeated singular (eigen) values, then each singular (eigen) vector is determined only up to a sign ambiguity. However, if XX^\top has repeated eigenvalues, then the singular (eigen) vectors corresponding to each repeated singular value are only unique up to an orthogonal transformation in the dimension of the corresponding subspace. Since one only observes two different adjacency matrices, then the leading singular vectors may not be aligned *a priori*. If one assumes that XX^\top has distinct eigenvalues, this sign ambiguity is often adjusted for by flipping the signs of each dimensions such that the medians have the same sign; that is for each embedding dimension, $\text{sign}(\text{median}(X_i)) = \text{sign}(\text{median}(Y_i))$ for all $i \in d$ [6, 25]. This heuristic can perform poorly when the medians of the samples are too close to zero. In addition, this approach falls short in the case of repeated eigenvalues of the matrix XX^\top since the subspace associated with such values are only unique up to a more general rotation, and hence the leading singular vectors of each adjacency matrix may not be close, even if n is large, since the leading singular values of the adjacency matrices will be perturbed versions of the singular values of XX^\top . For more details and discussion on this form of nonidentifiability, see Agterberg et al. [27].

If the two graphs had paired vertices, then the orthogonal misalignment between the two samples could be resolved by using a solution to a well-known orthogonal Procrustes problem [28]. In unpaired graphs, there is no *a priori* assignment between vertices, so we can employ an Optimal Transport Procrustes (OTP) algorithm [15], which simultaneously solves the alignment and the assignment problems. Formally, this algorithm minimizes the objective function

$$(2.1) \quad \min_{W, \Pi} \langle \Pi, C_W \rangle$$

where the entries of the cost matrix C_W are given by $(C_W)_{ij} = \|\hat{X}_i - W\hat{Y}_j\|^2$, $\hat{X} \in \mathbb{R}^{n \times d}$ and $\hat{Y} \in \mathbb{R}^{m \times d}$ are estimated latent positions, $\Pi = \frac{1}{nm} \mathbf{1}\mathbf{1}^\top$ is an assignment matrix that satisfies $\Pi \mathbf{1} = \frac{1}{n} \mathbf{1}$ and $\Pi^\top \mathbf{1} = \frac{1}{m} \mathbf{1}$, and W is constrained to be orthogonal. Given an initial guess W_0 , the algorithm iteratively updates $\Pi_{i+1}|W_i$ by via an optimal transport algorithm [29] and $W_{i+1}|\Pi_i$ using the solution to the Procrustes problem. In graph setting, the algorithm is initialized with all possible orthogonal diagonal matrices, i.e. the 2^d different diagonal matrices with ± 1 on the diagonal [15]. In Agterberg et al. [15], the authors show that the orthogonal matrix that globally minimizes the objective function (2.1) yields a consistent estimate of the orthogonal matrix approximately aligning the empirical distributions of the two ASEs, including when the corresponding graphs have (asymptotically) repeated singular (eigen) values.

2.3 Distance Correlation Due to the equivalence between two-sample and independence testing [17], distance correlations (DCorr) can be used to test the equality of the distributions F_X and F_Y . Define $Z = (X^\top, Y^\top)^\top \in \mathbb{R}^{N \times d}$ and $E = (0_n, 1_m)^\top \in \mathbb{R}^N$, where $N = n + m$. DCorr tests the

independence of Z and E using some distance functions $\delta_Z : \mathbb{R}^d \times \mathbb{R}^d \rightarrow \mathbb{R}$ and $\delta_E : \mathbb{R} \times \mathbb{R} \rightarrow \mathbb{R}$. First, DCorr computes distance matrices D^Z, D^E such that $D_{i,j}^Z = \delta_Z(Z_i, Z_j)$ and $D_{i,j}^E = \delta_E(E_i, E_j)$. The distance matrices are then doubly centered to $D^{Z'}, D^{E'}$, where $D_{i,j}^{Z'} = D_{i,j}^Z - \overline{D^Z}_{\cdot,j} - \overline{D^Z}_{i,\cdot} + \overline{D^Z}_{\cdot,\cdot}$, and similarly for $D^{E'}$. Here the column means, row means, and the grand mean are $\overline{D^Z}_{\cdot,j} = \frac{1}{N} \sum_{i=1}^N D_{i,j}^Z$, $\overline{D^Z}_{i,\cdot} = \frac{1}{N} \sum_{j=1}^N D_{i,j}^Z$, and $\overline{D^Z}_{\cdot,\cdot} = \frac{1}{N^2} \sum_{i=1}^N \sum_{j=1}^N D_{i,j}^Z$, respectively. The sample DCorr test statistic [30] is defined as

$$\text{DCorr}(Z, E) = \frac{1}{N(N-3)\sigma_{D^{Z'}}\sigma_{D^{E'}}} \sum_{i,j} D_{i,j}^{Z'} D_{i,j}^{E'}$$

where $\sigma_{D^{Z'}}$ and $\sigma_{D^{E'}}$ are the standard deviation of values in $D^{Z'}$ and $D^{E'}$, respectively. A null distribution of this test statistic can be generated by permuting the indices of E or approximated using an asymptotic result [31].

The centered versions $D^{Z'}, D^{E'}$ have the property that all rows and columns sum to zero, but the test statistic is biased for finite samples. An unbiased version of DCorr modifies the centering method of the pairwise distance matrices [30]. This method, called U-centering, generates a matrix $D^{Z''}$ that has the additional property that $E[D_{i,j}^{Z''}] = 0, i, j = 1, \dots, N$. $D^{Z''}$ uses a slightly different form for the row means, column means, and grand mean, given by $\widetilde{D^Z}_{\cdot,j} = \frac{1}{N-2} \sum_{i=1}^N D_{i,j}^Z$ (similarly for row means) and $\widetilde{D^Z}_{i,\cdot} = \frac{1}{(N-2)(N-1)} \sum_{i,j} D_{i,j}^Z$. The test statistic is defined analogously modulo these new definitions.

2.4 Multiscale Graph Correlation An alternative method for approaching the hypothesis testing problem is MGC [18–20], which uses the distance-based methods in DCorr, but also considers the local scale of the data. MGC is based on unbiased DCorr, resulting in it also being unbiased. MGC consists of the following steps.

1. Compute the centered distance matrices $D^{Z''}$ and $D^{E''}$.
2. For each k, l in $1, \dots, N$, compute the k and l nearest neighbors of each row of $D^{Z''}$ and $D^{E''}$, respectively, and denote the induced nearest neighbor graphs by $G^k \in \{0, 1\}^{N \times N}$ and $H^l \in \{0, 1\}^{N \times N}$.
3. Estimate the local normalized correlations $c^{k,l}$ such that

$$c^{kl} = \frac{\sum_{i,j} D_{i,j}^{Z''} D_{i,j}^{E''} G_{i,j}^k H_{i,j}^l}{\left(\sum_{i,j} (D_{i,j}^{Z''})^2 G_{i,j}^k \right) \left(\sum_{i,j} (D_{i,j}^{E''})^2 H_{i,j}^l \right)}.$$

4. Using a smoothing parameter τ , estimate the smoothed maximum of c^{kl} over all possible values of k and l , defined as

$$R = \text{LCC}\{(k, l) : c^{kl} > \max(\tau, c^{NN})\},$$

$$c^* = \max_{(k,l) \in R} c^{kl},$$

where LCC denotes the largest connected component of the graph defined by a set of edges.

Once the MGC test statistic c^* is obtained, a permutation test is performed to determine the null distribution. When the relationship is nonlinear or non-monotonic, MGC tends to choose scales smaller than n , detecting relationships more often than DCorr, and thus, it can be considered a direct generalization to the above methods, with often large finite sample power gains, with a minor running time cost [18].

3 Simulations The performance of DCorr and MGC is analyzed by simulating graphs with different distributions. The graphs are simulated according to the RDPG model, using different distributions (described below) to generate their univariate latent positions $X = (x_1, \dots, x_n)^\top$ and $Y = (y_1, \dots, y_n)^\top$, and the latent positions are estimated via ASE with embedding dimension $\hat{d} = 1$. The sign ambiguity is resolved via median flip since the graphs are embedded into one dimension. The estimates are then used to compute the corresponding test statistics, and calculate the p -value after estimating the null distribution via permutation test. The tests reject at a significance level $\alpha = 0.05$, and the empirical power is based on 1000 Monte Carlo replicates. This process is repeated for increasing numbers of vertices in each graph. The graph generating mechanisms are described next.

Equal distribution of the latent positions First, we analyze the performance of the methods when the null hypothesis is true, so the latent positions X and Y have the same distribution: $x_i \stackrel{\text{iid}}{\sim} F_X$ and $y_i \stackrel{\text{iid}}{\sim} F_X$, $i = 1, \dots, n$, with $F_X = \text{Unif}(.2, .7)$. That is, these mutually independent sets of latent positions are uniformly distributed on the range $(.2, .7)$. Figure 1 (left) shows the empirical size of the tests for different numbers of vertices. The empirical power does not exceed α , showing that both DCorr and MGC correctly control the type I error.

Linear difference in the distributions For this setting, we generate $x_i \stackrel{\text{iid}}{\sim} F_X$ and $y_i \stackrel{\text{iid}}{\sim} F_X + 0.1$ (Figure 1, middle). As the number of vertices in each graph increases, the difference between the distributions becomes easier to detect, and both DCorr and MGC algorithms detect the differences, resulting in power increasing to unity at equal rate for both methods.

Nonlinear difference in the distributions Finally, set $x_i \stackrel{\text{iid}}{\sim} F_X$ and $y_i \stackrel{\text{iid}}{\sim} 0.5 \text{Beta}(.2, .2) + 0.2$. Figure 1 (right) shows the power of both DCorr and MGC goes to 1, but MGC dominates DCorr at all sample sizes until both tests achieve power one..

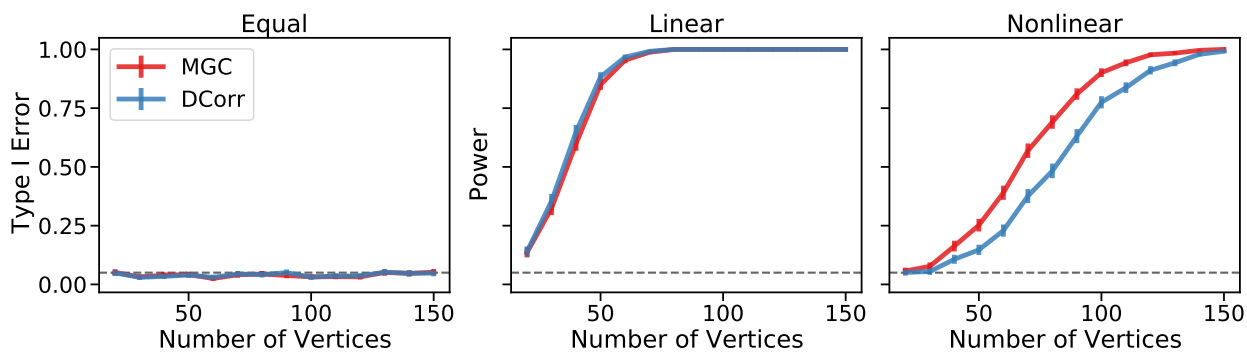


Figure 1: Type I error and power vs. number of vertices (n) for detecting differences in the distribution of latent positions using different methods (DCorr and MGC). Dashed lines represent $\alpha = 0.05$, and error bars represent 95% confidence interval. (Left) When the distributions of the latent positions are identical, both methods are valid as power is near or at $\alpha = 0.05$. (Middle) When the distributions are linearly dependent, both methods are equally powerful and consistent. (Right) When the distributions are nonlinearly dependent, both methods are consistent, but MGC is more powerful than DCorr.

4 Synthetic and Real Data Applications

Drosophila melanogaster brain The connectomes, or brain graphs, of the *Drosophila melanogaster* mushroom body have been obtained in Eichler et al. [32]. The left brain graph (A^L) has $n = 163$ neurons represented with the vertices, and the right brain graph (A^R) has $m = 158$ neurons. Both graphs are binary with $A_{ij} \in \{0, 1\}$, symmetric with $A = A^\top$, and hollow with $\text{diag}(A) = \vec{0}$. The edges of the data represent whether a synaptic connection exist between a pair of neurons or not.

Synthetic Data Analysis The performances of the two SVD alignment methods (median flipping and Optimal Transport Procrustes) and two hypothesis tests (DCorr and MGC) are analyzed by simulating synthetic data from the *Drosophila* connectomes. Given an estimated latent position matrix $\hat{X} \in \mathbb{R}^{n \times d}$ obtained from one of the hemispheres (either A^L or A^R), a pair of new latent position matrices are sampled, either with or without perturbation, to analyze the power and validity of various methods as a function of the number of vertices and the effect size.

The first step in data generation is to sample with replacement a set of m vertices from the original graph. Let $\mathcal{P} \subseteq [n]$ be the set of indices for the randomly selected vertices, where $|\mathcal{P}| = m$. For each $i \in \mathcal{P}$, a pair of d -dimensional random latent positions Y_i and Z_i are independently generated via

$$Y_i \sim \mathcal{MVN}(\hat{X}_i, \hat{\Sigma}(\hat{X}_i)), \quad Z_i \sim \mathcal{MVN}(\hat{X}_i + \epsilon_i, \hat{\Sigma}(\hat{X}_i)),$$

where $\mathcal{MVN}(x, \Sigma)$ is a d -variate normal distribution with mean x and covariance Σ , and $\hat{\Sigma}(\hat{X}_i)$ is the covariance matrix of the difference between \hat{X}_i and X_i given by the central limit theorem in Athreya et al. [33], which is introduced to account for the fact that the true latent position X_i is not observed. A random subset $\mathcal{O} \subseteq \mathcal{P}$ of the vertices are perturbed by adding ϵ_i , defined as

$$\epsilon_j \sim \begin{cases} \text{Unif}(S_r^d), & \text{if } j \in \mathcal{O} \\ \vec{0}, & \text{otherwise,} \end{cases}$$

where $\text{Unif}(S_r^d)$ is the uniform distribution on the surface of a d dimensional sphere with radius r . Thus, r represents the effect size, and $\rho = |\mathcal{O}|/m$ is the proportion of changed vertices. Given the new latent position matrices Y and Z , a pair of undirected graphs A and B are generated by sampling the edges independently as $A_{ij} \sim \text{Bernoulli}(\min\{1, \max\{0, Y_i^\top Y_j\}\})$ and $B_{ij} \sim \text{Bernoulli}(\min\{1, \max\{0, Z_i^\top Z_j\}\})$, for $i > j$. A and B are symmetrized by setting $A_{ij} = A_{ji}$ and $B_{ij} = B_{ji}$.

Once the new adjacency matrices A and B are sampled, we test the hypothesis that the distributions used to generate their latent positions are the same. The hypotheses are rejected at a significance level $\alpha = 0.05$, and the empirical power based on 500 Monte Carlo replicates is reported. This process is repeated for increasing number of vertices with $m \in [20, 200]$, and proportion of changed vertices with $\rho \in \{0, 0.5, 1\}$, while keeping the effect size constant with $r = 1$ for both left and right *Drosophila* mushroom body.

Figure 2 shows that aligning the latent positions via the median flip yields invalid results for both DCorr and MGC. Specifically, when $\rho = 0$, both Y and Z are sampled from the same distribution, but both DCorr and MGC yield type I errors greater than 0.05 via median flip. The OTP alignment resolves the invalidity of the median flip as power is near $\alpha = 0.05$. In addition, when $\rho > 0$, the empirical power for both DCorr and MGC using OTP increases as the the sample size and proportion of vertices changed increases, showing that both methods are able to identify a significant difference between the distributions. Lastly, the MGC test statistic is more powerful than the DCorr test statistic in all scenarios where $\rho > 0$.

Left vs Right Larval Drosophila Mushroom Body The left and right *Drosophila* mushroom body are similar, but not identical. To compare these hemispheres, we test the difference of the distributions of

the graph of the left mushroom body (L) and the graph of the right mushroom body (R). The ASE of each hemisphere are denoted by \hat{X}_L and \hat{X}_R , estimating latent positions of RDPG models for each hemisphere, with assumed distributions F_L and F_R respectively. We test the hypothesis $H_0 : F_L = F_R$ vs $H_1 : F_L \neq F_R$. Figure 3 shows pair-plots of the embeddings after alignment with OTP and median flip. Using the estimated latent positions, we test the equality of the distributions using the same methods as before. The p -values are shown in Table 1. As observed in Figure 3, the latent positions of both hemispheres are similar, suggesting there is no difference in the distributions. However, median flip fails due to misalignment in one of the embedding dimensions, resulting in $p < 0.01$, while testing and aligning via OTP results in $p \approx 1$.

5 Discussion The results presented herein demonstrate the improvement of the nonparametric two-sample graph testing presented in Tang et al. [6] by aligning estimated latent positions via Optimal Transport Procrustes (OTP) and testing via multiscale graph correlation. For applications in connectomics, we show that the orthogonal nonidentifiabilities that arise from adjacency spectral embedding can significantly impacts the results. Specifically, the synthetic data experiments show that median flip can invalidate DCorr and MGC, but OTP resolves the inadequacy of median flip. Both simulated and synthetic experiments show that MGC is more powerful than DCorr when testing via OTP. Thus, testing via OTP and MGC is not only more powerful, but also more trustworthy. While this work focuses on cases where the two graphs have the same number of vertices, the testing procedure can be extended to cases where the two networks have different number of vertices by correcting the variance of the estimated latent positions [25].

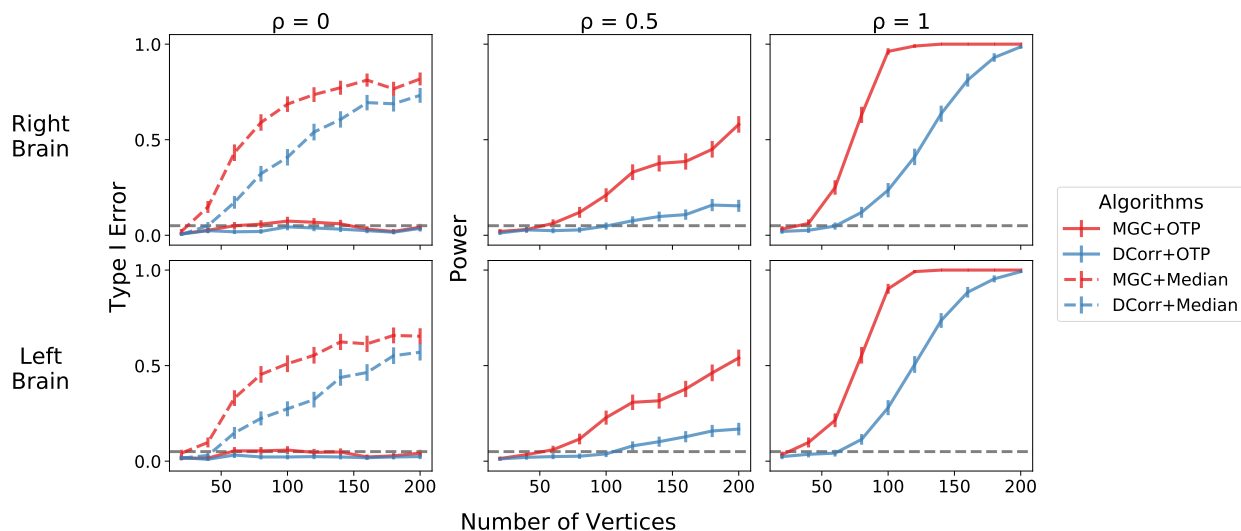


Figure 2: Type I error and power vs. number of vertices (n) using synthetic data generated from *Drosophila* connectomes. The effect size, or the magnitude of the change in latent positions, is fixed at $r = 1$. The gray dashed line is $\alpha = 0.05$. Each row represents right or left hemisphere of the brain, and each column represents different proportion of vertices changed. When $\rho = 0$, the latent position distributions F_V and F_W are the same. Latent position alignment via median flip is invalid as shown in first column ($\rho = 0$) as type I error is above α and increasing with the size of the graphs; OTP resolves the invalidity of median flip. Testing via MGC is more powerful than testing via DCorr as shown in columns where $\rho = 0.5$ and $\rho = 1$. Curves for median flip testing are omitted in the middle and right panels since using median flip results in an invalid test.

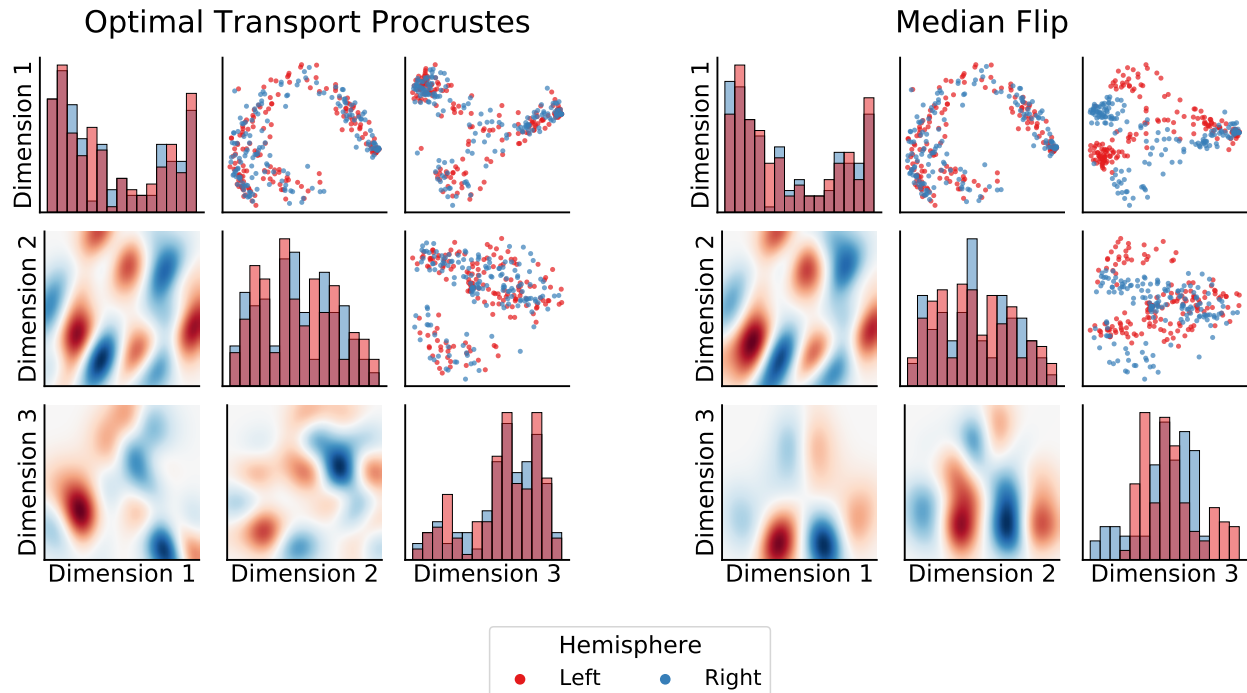


Figure 3: Embeddings for the *Drosophila* connectomes after alignment with Optimal Transport Procrustes (left) and median flip (right). The diagonals are histograms of each dimension, upper off-diagonals are pairwise scatter plots, and lower off-diagonals are the difference of the kernel density estimates of the two embeddings. (Left) OTP aligns all three dimensions properly. (Right) Median flips results in misalignment in dimension 3 of the left hemisphere embedding.

Algorithm	p -value	Successful Alignment
MGC+OTP	0.9982	✓
DCorr+OTP	0.9978	✓
MGC+Median	0.0001	✗
DCorr+Median	0.001	✗

Table 1: P-values from testing the for differences in distribution of the left and right *Drosophila* mushroom body, specifically $H_0 : F_L = F_R$ vs $H_1 : F_L \neq F_R$. At $\alpha = 0.05$, testing via optimal transport Procrustes does not reject the null hypothesis, but testing via median flip rejects the null hypothesis when it should not. Last column shows whether the alignment of the latent positions succeeded or not.

6 Code The analysis were performed using the `graspologic` [34] and `hyppo` [35] Python packages. The methods described herein are implemented in `graspologic`.

Acknowledgment The authors would like to thank the NeuroData group for great advice and an equally great working environment. This material is based on research sponsored by the Defense Advanced Research Projects Agency (DARPA) Lifelong Learning Machines program [grant number FA8650-18-2-7834], the National Science Foundation award [grant number DMS-1921310], the Air

Force Research Laboratory and DARPA [grant number FA8750-20-2-1001], and funding from Microsoft Research. The U.S. Government is authorized to reproduce and distribute reprints for Governmental purposes notwithstanding any copyright notation thereon. The views and conclusions contained herein are those of the authors and should not be interpreted as necessarily representing the official policies or endorsements, either expressed or implied, of the Air Force Research Laboratory and DARPA or the U.S. Government

References

- [1] Anna Goldenberg, Alice X. Zheng, Stephen E. Fienberg, and Edoardo M. Airoldi. A survey of statistical network models. *Found. Trends Mach. Learn.*, 2(2):129–233, February 2010. ISSN 1935-8237. doi: 10.1561/22000000005. URL <http://dx.doi.org/10.1561/2200000005>.
- [2] Ed Bullmore and Olaf Sporns. Complex brain networks: graph theoretical analysis of structural and functional systems. *Nature reviews neuroscience*, 10(3):186, 2009.
- [3] Stanley Wasserman, Katherine Faust, et al. *Social network analysis: Methods and applications*, volume 8. Cambridge university press, 1994.
- [4] Minh Tang, Avanti Athreya, Daniel L. Sussman, Vince Lyzinski, Youngser Park, and Carey E. Priebe. A semiparametric two-sample hypothesis testing problem for random graphs. *Journal of Computational and Graphical Statistics*, 26(2):344–354, 2017. doi: 10.1080/10618600.2016.1193505. URL <https://doi.org/10.1080/10618600.2016.1193505>.
- [5] K. Levin, A. Athreya, M. Tang, V. Lyzinski, and C. E. Priebe. A central limit theorem for an omnibus embedding of multiple random dot product graphs. In *2017 IEEE International Conference on Data Mining Workshops (ICDMW)*, pages 964–967, 2017. doi: 10.1109/ICDMW.2017.132.
- [6] Minh Tang, Avanti Athreya, Daniel L. Sussman, Vince Lyzinski, and Carey E. Priebe. A nonparametric two-sample hypothesis testing problem for random graphs. *Bernoulli*, 23(3):1599–1630, 08 2017. doi: 10.3150/15-BEJ789. URL <https://doi.org/10.3150/15-BEJ789>.
- [7] Debarghya Ghoshdastidar, Maurilio Gutzeit, Alexandra Carpentier, and Ulrike von Luxburg. Two-sample tests for large random graphs using network statistics. In Satyen Kale and Ohad Shamir, editors, *Proceedings of the 2017 Conference on Learning Theory*, volume 65 of *Proceedings of Machine Learning Research*, pages 954–977, Amsterdam, Netherlands, 07–10 Jul 2017. PMLR. URL <http://proceedings.mlr.press/v65/ghoshdastidar17a.html>.
- [8] Keith Levin and Elizaveta Levina. Bootstrapping networks with latent space structure, 2019. arXiv:1907.10821.
- [9] Jesús Arroyo, Avanti Athreya, Joshua Cape, Guodong Chen, Carey E. Priebe, and Joshua T. Vogelstein. Inference for multiple heterogeneous networks with a common invariant subspace, 2019.
- [10] Andrey Rukhin and Carey E. Priebe. A comparative power analysis of the maximum degree and size invariants for random graph inference. *Journal of Statistical Planning and Inference*, 141(2): 1041 – 1046, 2011. ISSN 0378-3758. doi: <https://doi.org/10.1016/j.jspi.2010.09.013>. URL <http://www.sciencedirect.com/science/article/pii/S0378375810004246>.
- [11] Dena Marie Asta and Cosma Rohilla Shalizi. Geometric network comparisons. In *Proceedings of the Thirty-First Conference on Uncertainty in Artificial Intelligence, UAI’15*, pages 102–110, Arlington, Virginia, United States, 2015. AUAI Press. ISBN 978-0-9966431-0-8. URL <http://dl.acm.org/citation.cfm?id=3020847.3020859>.
- [12] P.-A. G. Maugis, S. C. Olhede, C. E. Priebe, and P. J. Wolfe. Testing for equivalence of network distribution using subgraph counts. *Journal of Computational and Graphical Statistics*, 0(0):1–11, 2020. doi: 10.1080/10618600.2020.1736085. URL <https://doi.org/10.1080/10618600.2020>.

1736085.

- [13] Debarghya Ghoshdastidar, Maurilio Gutzeit, Alexandra Carpentier, and Ulrike von Luxburg. Two-sample hypothesis testing for inhomogeneous random graphs, 2019. arXiv:1707.00833.
- [14] Cedric E Ginestet, Jun Li, Prakash Balachandran, Steven Rosenberg, and Eric D. Kolaczyk. Hypothesis testing for network data in functional neuroimaging. *Annals of Applied Statistics*, 11(2): 725–750, 2017. ISSN 19417330. doi: 10.1214/16-AOAS1015. URL <https://projecteuclid.org/download/pdfview/1/euclid.aos/1500537721>.
- [15] Joshua Agterberg, Minh Tang, and Carey Priebe. Nonparametric two-sample hypothesis testing for random graphs with negative and repeated eigenvalues. *arXiv preprint arXiv:2012.09828*, 2020.
- [16] Cencheng Shen and Joshua T. Vogelstein. The exact equivalence of distance and kernel methods for hypothesis testing, 2018. arXiv:1806.05514.
- [17] Cencheng Shen, Carey E. Priebe, and Joshua T. Vogelstein. The exact equivalence of independence testing and two-sample testing, 2019. arXiv:1910.08883.
- [18] J. T. Vogelstein, Q. Wang, E. Bridgeford, C. E. Priebe, M. Maggioni, and C. Shen. Discovering and deciphering relationships across disparate data modalities. *eLife*, 8:e41690, 2019.
- [19] C. Shen, C. E. Priebe, and J. T. Vogelstein. From distance correlation to multiscale graph correlation. *Journal of the American Statistical Association*, 2019.
- [20] Y. Lee, C. Shen, C. E. Priebe, and J. T. Vogelstein. Network dependence testing via diffusion maps and distance-based correlations. *Biometrika*, 2019.
- [21] Avanti Athreya, Donniell E. Fishkind, Minh Tang, Carey E. Priebe, Youngser Park, Joshua T. Vogelstein, Keith Levin, Vince Lyzinski, Yichen Qin, and Daniel L Sussman. Statistical inference on random dot product graphs: a survey. *Journal of Machine Learning Research*, 18(226):1–92, 2018. URL <http://jmlr.org/papers/v18/17-448.html>.
- [22] Daniel L. Sussman, Minh Tang, Donniell E. Fishkind, and Carey E. Priebe. A consistent adjacency spectral embedding for stochastic blockmodel graphs. *Journal of the American Statistical Association*, 107(499):1119–1128, 2012. doi: 10.1080/01621459.2012.699795. URL <https://doi.org/10.1080/01621459.2012.699795>.
- [23] Daniel Sussman, Minh Tang, and Carey Priebe. Consistent latent position estimation and vertex classification for random dot product graphs. *IEEE Transactions on Pattern Analysis and Machine Intelligence*, 36:48–57, 2014. doi: 10.1109/TPAMI.2013.135.
- [24] Vince Lyzinski, Daniel L. Sussman, Minh Tang, Avanti Athreya, and Carey E. Priebe. Perfect clustering for stochastic blockmodel graphs via adjacency spectral embedding. *Electronic Journal of Statistics*, 8(2):2905–2922, 2014. doi: 10.1214/14-EJS978. URL <https://doi.org/10.1214/14-EJS978>.
- [25] Anton A. Alyakin, Joshua Agterberg, Hayden S. Helm, and Carey E. Priebe. Correcting a nonparametric two-sample graph hypothesis test for graphs with different numbers of vertices, 2020.
- [26] Mu Zhu and Ali Ghodsi. Automatic dimensionality selection from the scree plot via the use of profile likelihood. *Computational Statistics & Data Analysis*, 51(2):918–930, 2006.
- [27] Joshua Agterberg, Minh Tang, and Carey E. Priebe. On two distinct sources of nonidentifiability in latent position random graph models, 2020. arXiv:2003.14250.
- [28] Peter H Schönemann. A generalized solution of the orthogonal procrustes problem. *Psychometrika*, 31(1):1–10, 1966.
- [29] David Alvarez-Melis, Stefanie Jegelka, and Tommi S Jaakkola. Towards optimal transport with global invariances. pages 1870–1879, 2019.
- [30] G. Székely and M. Rizzo. Partial distance correlation with methods for dissimilarities. *Annals of*

- Statistics, 42(6):2382–2412, 2014.
- [31] Cencheng Shen and Joshua T Vogelstein. The chi-square test of distance correlation. arXiv preprint arXiv:1912.12150, 2019.
 - [32] Katharina Eichler, Feng Li, Ashok Litwin-Kumar, Youngser Park, Ingrid Andrade, Casey M Schneider-Mizell, Timo Saumweber, Annina Huser, Claire Eschbach, Bertram Gerber, et al. The complete connectome of a learning and memory centre in an insect brain. Nature, 548(7666):175, 2017.
 - [33] A Athreya, C E Priebe, M Tang, V Lyzinski, D J Marchette, and D L Sussman. A Limit Theorem for Scaled Eigenvectors of Random Dot Product Graphs. Technical report, 2015.
 - [34] Jaewon Chung, Benjamin D. Pedigo, Eric W. Bridgeford, Bijan K. Varjavand, Hayden S. Helm, and Joshua T. Vogelstein. Grasp: Graph statistics in python. Journal of Machine Learning Research, 20(158):1–7, 2019. URL <http://jmlr.org/papers/v20/19-490.html>.
 - [35] Sambit Panda, Satish Palaniappan, Junhao Xiong, Eric W. Bridgeford, Ronak Mehta, Cencheng Shen, and Joshua T. Vogelstein. hyppo: A comprehensive multivariate hypothesis testing python package. 2020.